Spectrum Sharing between Cooperative Relay and Ad-hoc Networks: Dynamic Transmissions under Computation and Signaling Limitations

Yin Sun, Xiaofeng Zhong, Yunzhou Li, Shidong Zhou and Xibin Xu
State Key Laboratory on Microwave and Digital Communications
Tsinghua National Laboratory for Information Science and Technology
Department of Electronic Engineering, Tsinghua University, Beijing, 100084, China.
E-mail: sunyin02@gmail.com, {zhongxf,liyunzhou,zhousd,xuxb}@tsinghua.edu.cn.

***Abstract*—This paper studies a spectrum sharing scenario between a cooperative relay network (CRN) and a nearby ad-hoc network. In particular, we consider a dynamic spectrum access and resource allocation problem of the CRN. Based on sensing and predicting the ad-hoc transmission behaviors, the ergodic traffic collision time between the CRN and ad-hoc network is minimized subject to an ergodic uplink throughput requirement for the CRN.**

We focus on real-time implementation of spectrum sharing policy under practical computation and signaling limitations. In our spectrum sharing policy, most computation tasks are accomplished off-line. Hence, little real-time calculation is required which fits the requirement of practical applications. Moreover, the signaling procedure and computation process are designed carefully to reduce the time delay between spectrum sensing and data transmission, which is crucial for enhancing the accuracy of traffic prediction and improving the performance of interference mitigation. The benefits of spectrum sensing and cooperative relay techniques are demonstrated by our numerical experiments.

***Index Terms*—Ad-hoc Network; Cooperative Relay Network; Spectrum Access; Traffic prediction; Resource Allocation; Real-time Implementation.**

I. INTRODUCTION

In recent years, spectrum sharing between heterogeneous wireless networks has been studied intensively as a crucial technology for improving network spectrum efficiency [1] and network capacity [2]. Traffic prediction based spectrum access polices were proposed in [3]–[9], where the cognitive transmitter detects and predicts the primary user's (PU) transmission behaviors and transmits signals opportunistically to avoid collisions with the PU's traffic. Joint optimization of spectrum access and resource allocation based on traffic prediction has been proposed in [10] for an open sharing model [1] that considers spectrum sharing between an uplink system and an ad-hoc network. In [11], cooperative relay technique was utilized to improve the spectrum sharing performance.

However, some implementation issues were rarely considered in these studies. First, determining the resource allocation policy in real-time can be computationally quite demanding for realistic wireless communication systems [12]. Second, spectrum sensing and channel estimation are usually performed at spatially separate nodes, which requires to exchange their obtained information before solve the resource allocation problem. The resultant signaling procedure and the computation of resource allocation solution would cause a large time delay between spectrum sensing and data transmission, which would degrade the accuracy of traffic prediction and cause unexpected traffic collisions between the networks operating in the same spectrum. Therefore, resource allocation policies with little real-time calculation and small sensing-transmission delay are of great interest for practical applications.

In this paper, we study spectrum sharing between a cooperative relay network (CRN) and an ad-hoc network, as illustrated in Fig. 1. The relay assists the transmissions from the mobile terminal (MT) to the base station (BS) to achieve higher uplink throughput. In order to communicate with the distant BS, the MT and relay would transmit signals with peak powers, which induce strong interference to nearby ad-hoc links. The ad-hoc transmitters (e.g., wireless sensor nodes) have relative low transmission powers due to their short communication ranges, and thus their interference to the relay and BS can be treated as noise. Such an asymmetrical interference scenario is known as the "near-far effect" [2].

We consider a joint spectrum access and resource allocation problem of the CRN, where the ergodic traffic collision time between the CRN and ad-hoc network is minimized subject to an ergodic uplink throughput constraint for the CRN. The formulated design problem is a difficult nonconvex optimization problem with no closed-form expression for the objective function. By carefully analyzing the problem structure, we show how this problem can be reformulated as a convex problem. A low-complexity Lagrangian optimization method is used to solve the considered design problem efficiently. Then, a real-time implementation policy is proposed which requires little real-time calculation and has small sensing-transmission delay. Finally, numerical results are provided to show the benefits of our spectrum sharing policy.

II. SYSTEM MODEL

The CRN operates in frames with duration T_f. Each frame comprises N sub-channels in frequency domain, denoted by

This work was supported by National S&T Major Project (2008ZX03O03-004), National Basic Research Program of China (2007CB310608), China's 863 Project (2009AA011501), National Natural Science Foundation of China (60832008) and Tsinghua-Qualcomm Joint Research Program.

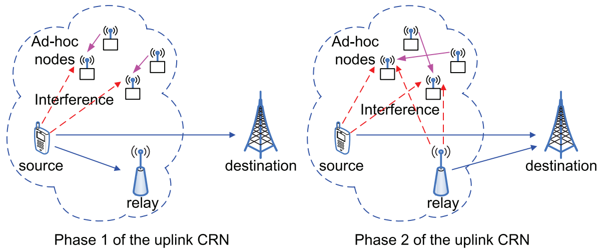

Fig. 1: System setup of the spectrum sharing between cooperative relay and ad-hoc networks.

the set $\mathcal{N} = \{1, 2, \cdots, N\}$. We assume that the wireless channels of source-relay (S-R), source-destination (S-D), and relay-destination (R-D) links are block-faded, which vary across the frames in a stationary and ergodic manner. The channel gain normalized by the interference plus noise power of these links are denoted by $g_n^{s,r}, g_n^{r,d}, g_n^{s,d}$, respectively, for the n-th sub-channel.

In practice, the relay node operates in a half-duplex mode. Therefore, each frame consists of 2 phases: In Phase 1, the source transmits signal to the relay and destination via a broadcast channel; in Phase 2, the source transmits a new information message, and, at the same time, the relay uses the DF relaying strategy to forward its received information message in Phase 1 to the destination, which forms a multiple-access channel. These operations are illustrated in Fig. 1. The time durations of Phase 1 and Phase 2 are set to αT_f and $(1-\alpha)T_f$, respectively, where $\alpha \in (0, 1)$.

The ad-hoc links operate in M non-overlapping frequency bands denoted by the set $\mathcal{M} = \{1, 2, \cdots, M\}$ and the m-th ad-hoc band overlaps with a set of sub-channels given by $\mathcal{N}_m$ ($\mathcal{N} = \bigcup_{m=1}^{M} \mathcal{N}_m$ and $\mathcal{N}_m \bigcap \mathcal{N}_l = \emptyset$ if $m \neq l$). The ad-hoc traffic in the m-th band is modeled by a strictly stationary, ergodic and independent binary continuous-time Markov chain (CTMC) $X_m(t)$, where $X_m(t) = 1$ ($X_m(t) = 0$) represents an ACTIVE (IDLE) state at time t. The holding (or sojourn) periods of ACTIVE and IDLE states are exponentially distributed with rate parameters λ and μ, respectively. The probability transition matrix of the CTMC model of Band m is given by [13, p. 391]

$$P(t) = \frac{1}{\lambda+\mu}\begin{bmatrix} \mu+\lambda e^{-(\lambda+\mu)t} & \lambda-\lambda e^{-(\lambda+\mu)t} \\ \mu-\mu e^{-(\lambda+\mu)t} & \lambda+\mu e^{-(\lambda+\mu)t} \end{bmatrix}, \tag{1}$$

where the element in the $(i+1)$-th row and $(j+1)$-th column of $P(t)$ stands for the transition probability $\Pr\{X_m(t+\tau) = j | X_m(\tau) = i\}$ for $i, j \in \{0, 1\}$. This CTMC model has been considered in many spectrum sharing studies including theoretical analysis and hardware tests; see [3]–[11].

The source and relay detect the ACTIVE/IDLE state of each ad-hoc band at the start of both Phase 1 and Phase 2. The sensing outcome of the two phases are denoted by $X_m(0) = x_m \in \{0, 1\}$ and $X_m(\alpha T_f) = y_m \in \{0, 1\}$, respectively. Perfect sensing and negligible sensing overhead are assumed in this paper.

III. Problem Formulation

Let us define $\boldsymbol{\omega} \triangleq \{g_n^{s,r}, g_n^{r,d}, g_n^{s,d}, x_m, y_m, n \in \mathcal{N}, m \in \mathcal{M}\}$ as the network state information (NSI). The dynamic transmission parameters are determined by the instant NSI $\boldsymbol{\omega}$. Suppose that the source and relay nodes can switch on and off their transmissions freely over each sub-channel, and may transmit only in part of the time during Phase 1 and Phase 2. Let $\mathbb{I}_n^{(1)}(\boldsymbol{\omega}) \subseteq [0, \alpha T_f]$ denote the set of transmission time of the source over Sub-channel n in Phase 1, and $\mathbb{I}_n^{(2)}(\boldsymbol{\omega}) \subseteq [\alpha T_f, T_f]$ denote that of the source and relay in Phase 2, for $n = 1, \ldots, N$. $\mathbb{I}_n^{(1)}(\boldsymbol{\omega})$ and $\mathbb{I}_n^{(2)}(\boldsymbol{\omega})$ each may be *a union of several disjoint transmission time intervals*. We utilize the words "traffic collision" to represent the event that both the CRN and ad-hoc network are transmitting in the same spectrum band at the same time. In [14], we showed that ergodic traffic collision time between the two networks is given as

$$\begin{aligned} \overline{I} = \mathbb{E}_{\boldsymbol{\omega}}\Bigg\{\sum_{m=1}^{M}\Bigg[&\int_{\bigcup_{n\in\mathcal{N}_m}\mathbb{I}_n^{(1)}(\boldsymbol{\omega})} \Pr\{X_m(\sigma) = 1 | X_m(0) = x_m\}\, d\sigma \\ &+ \int_{\bigcup_{n\in\mathcal{N}_m}\mathbb{I}_n^{(2)}(\boldsymbol{\omega})} \Pr\{X_m(\sigma) = 1 | X_m(\alpha T_f) = y_m\}\, d\sigma\Bigg]\Bigg\}, \end{aligned} \tag{2}$$

which is proportional to the transmission error probability of the ad-hoc network in strong interference scenarios [4].

Let $\pi(S)$ represents the size (measure) of set S; for example, $\pi([a, b]) = b - a$. Thus, the transmission time fractions of the CRN are determined as $\theta_n^{(1)}(\boldsymbol{\omega}) = \pi(\mathbb{I}_n^{(1)}(\boldsymbol{\omega}))/T_f$ and $\theta_n^{(2)}(\boldsymbol{\omega}) = \pi(\mathbb{I}_n^{(2)}/(\boldsymbol{\omega}))T_f$, respectively, for Phase 1 and Phase 2 of the frame. Then, the ergodic achievable rate of the CRN can be expressed as [14]

$$\begin{aligned} &\overline{R}_{DF} \\ &= W \min \sum_{n=1}^{N} \mathbb{E}_{\boldsymbol{\omega}}\Bigg[\theta_n^{(1)}(\boldsymbol{\omega}) \log_2\Bigg(1 + \frac{P_{s,n}^{(1)}(\boldsymbol{\omega}) \max\{g_n^{s,r}, g_n^{s,d}\}}{\theta_n^{(1)}(\boldsymbol{\omega})}\Bigg) \\ &\quad + \theta_n^{(2)}(\boldsymbol{\omega}) \log_2\Bigg(1 + \frac{P_{s,n}^{(2)}(\boldsymbol{\omega}) g_n^{s,d}}{\theta_n^{(2)}(\boldsymbol{\omega})}\Bigg)\Bigg], \\ &\quad \sum_{n=1}^{N} \mathbb{E}_{\boldsymbol{\omega}}\Bigg[\theta_n^{(1)}(\boldsymbol{\omega}) \log_2\Bigg(1 + \frac{P_{s,n}^{(1)}(\boldsymbol{\omega}) g_n^{s,d}}{\theta_n^{(1)}(\boldsymbol{\omega})}\Bigg) \\ &\quad + \theta_n^{(2)}(\boldsymbol{\omega}) \log_2\Bigg(1 + \frac{P_{s,n}^{(2)}(\boldsymbol{\omega}) g_n^{s,d} + P_{r,n}(\boldsymbol{\omega}) g_n^{r,d}}{\theta_n^{(2)}(\boldsymbol{\omega})}\Bigg)\Bigg]\Bigg\}. \end{aligned} \tag{3}$$

Note that this ergodic rate can be achieved in slow-fading environment by means of queuing at the relay node. Moreover, it is a concave function of $\{P_{s,n}^{(1)}(\boldsymbol{\omega}), P_{s,n}^{(2)}(\boldsymbol{\omega}), P_{r,n}(\boldsymbol{\omega}), \theta_n^{(1)}(\boldsymbol{\omega}), \theta_n^{(2)}(\boldsymbol{\omega}), n \in \mathcal{N}\}$, since the perspective of a concave function is also concave [15, p. 89].

The joint spectrum access and resource allocation problem the CRN is formulated as

$$(\mathsf{P}) \quad \min_{\substack{P_{s,n}^{(1)}(\boldsymbol{\omega}), P_{s,n}^{(2)}(\boldsymbol{\omega}), P_{r,n}(\boldsymbol{\omega}), \mathbb{I}_n^{(1)}(\boldsymbol{\omega}), \mathbb{I}_n^{(2)}(\boldsymbol{\omega}), \\ \theta_n^{(1)}(\boldsymbol{\omega}), \theta_n^{(2)}(\boldsymbol{\omega}),\ n=1,\ldots,N}} \overline{I} \tag{4}$$

$$\text{s.t. } \overline{R}_{DF} \geq R_{\min} \tag{5}$$

$$\mathbb{E}_{\boldsymbol{\omega}}\left\{\sum_{n=1}^{N}\left[P_{s,n}^{(1)}(\boldsymbol{\omega}) + P_{s,n}^{(2)}(\boldsymbol{\omega})\right]\right\} \leq P_{\max}^{s} \tag{6}$$

$$\mathbb{E}_{\boldsymbol{\omega}}\left\{\sum_{n=1}^{N} P_{r,n}(\boldsymbol{\omega})\right\} \leq P_{\max}^{r} \tag{7}$$

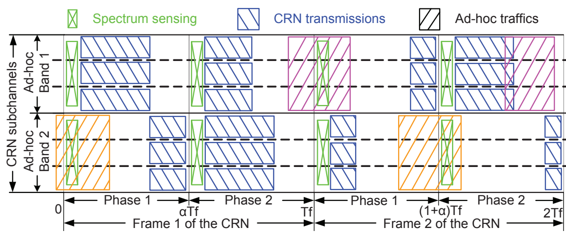

Fig. 2: Time-frequency transmission structure by Lemma 1.

$$P_{s,n}^{(1)}(\boldsymbol{\omega}), P_{s,n}^{(2)}(\boldsymbol{\omega}), P_{r,n}(\boldsymbol{\omega}) \geq 0 \tag{8}$$

$$\mathbb{I}_n^{(1)}(\boldsymbol{\omega}) \subseteq [0, \alpha T_f], \quad \mathbb{I}_n^{(2)}(\boldsymbol{\omega}) \subseteq [\alpha T_f, T_f] \tag{9}$$

$$\pi(\mathbb{I}_n^{(1)}(\boldsymbol{\omega})) = \theta_n^{(1)}(\boldsymbol{\omega}) T_f, \quad \pi(\mathbb{I}_n^{(2)}(\boldsymbol{\omega})) = \theta_n^{(2)}(\boldsymbol{\omega}) T_f. \tag{10}$$

IV. The solution to the problem (P)

Problem (P) is difficult to solve mainly because it is hard to determine the sets $\mathbb{I}_n^{(1)}(\boldsymbol{\omega})$ and $\mathbb{I}_n^{(2)}(\boldsymbol{\omega})$ and thus the objective function $\overline{I}$ has no closed-form expression in general. Fortunately, these issues can be resolved and eventually (P) can be reformulated as a convex optimization problem, as we present in the following.

A. Transformation of (P) to a convex problem

In [14], we show that the optimal spectrum access should satisfy the following two principles:

1) The source and relay nodes should transmit as soon (late) as possible if the sensing outcome is IDLE (ACTIVE);
2) The CRN should have identical spectrum access policy for all sub-channels in $\mathcal{N}_m$; that is, $\mathbb{I}_p^{(i)} = \mathbb{I}_q^{(i)}$ for all $p, q \in \mathcal{N}_m$ and $i \in \{1, 2\}$.

Let us define

$$\theta_m^{(i)}(\boldsymbol{\omega}) \triangleq \max\left\{\theta_n^{(i)}(\boldsymbol{\omega}), n \in \mathcal{N}_m\right\}, \tag{11}$$

for $m = 1, \ldots, M$ and $i = 1, 2$. The above principles are formalized in the following Lemma:

Lemma 1 *[14] For any given transmission time fractions $\{\theta_m^{(1)}(\boldsymbol{\omega}) \in [0, \alpha], \theta_m^{(2)}(\boldsymbol{\omega}) \in [0, 1-\alpha]\}_{m=1}^{M}$, we have that:*

1) The optimal spectrum access policy of Phase 1 is given by $\mathbb{I}_n^{(1)}(\boldsymbol{\omega}) = [0, \theta_m^{(1)}(\boldsymbol{\omega}) T_f]$ ($\mathbb{I}_n^{(1)}(\boldsymbol{\omega}) = [(\alpha - \theta_m^{(1)}(\boldsymbol{\omega})) T_f, \alpha T_f]$) for all $n \in \mathcal{N}_m$, if the sensing outcome of Phase 1 is $x_m = 0$ ($x_m = 1$);

2) The optimal spectrum access policy of Phase 2 is given by $\mathbb{I}_n^{(2)}(\boldsymbol{\omega}) = [\alpha T_f, (\alpha + \theta_m^{(2)}(\boldsymbol{\omega})) T_f]$ ($\mathbb{I}_n^{(2)}(\boldsymbol{\omega}) = [(1 - \theta_m^{(2)}(\boldsymbol{\omega})) T_f, T_f]$) for all $n \in \mathcal{N}_m$, if the sensing outcome of Phase 2 is $y_m = 0$ ($y_m = 1$),

An example of the spectrum access policy in Lemma 1 is shown in Fig. 2. According to Lemma 1, each term inside the expectation in (2) can be greatly simplified. For $\theta \in [0, \alpha]$, define the functions

$$\phi_{(1)}(\theta; 0) = \int_{[0, \theta T_f]} \Pr(X_m(t) = 1 | X_m(0) = 0) dt$$
$$= \frac{\lambda T_f}{\lambda + \mu} \left\{\theta + \frac{1}{(\lambda + \mu) T_f}\left[e^{-(\lambda+\mu)\theta T_f} - 1\right]\right\}, \tag{12}$$

$$\phi_{(1)}(\theta; 1) = \int_{[(\alpha-\theta)T_f, \alpha T_f]} \Pr(X_m(t) = 1 | X_m(0) = 1) dt$$
$$= \frac{\lambda T_f}{\lambda + \mu} \left\{\theta + \frac{\mu/\lambda}{(\lambda + \mu) T_f} e^{-(\lambda+\mu)\alpha T_f} \left[e^{(\lambda+\mu)\theta T_f} - 1\right]\right\}, \tag{13}$$

and for $\theta \in [0, \alpha]$, define the functions

$$\phi_{(2)}(\theta; 0) = \int_{[\alpha T_f, (\theta+\alpha) T_f]} \Pr(X_m(t) = 1 | X_m(\alpha T_f) = 0) dt$$
$$= \frac{\lambda T_f}{\lambda + \mu} \left\{\theta + \frac{1}{(\lambda + \mu) T_f}\left[e^{-(\lambda+\mu)\theta T_f} - 1\right]\right\}, \tag{14}$$

$$\phi_{(2)}(\theta; 1) = \int_{[T_f - \theta T_f, T_f]} \Pr(X_m(t) = 1 | X_m(\alpha T_f) = 1) dt$$
$$= \frac{\lambda T_f}{\lambda + \mu} \left\{\theta + \frac{\mu/\lambda}{(\lambda + \mu) T_f} e^{-(\lambda+\mu)(1-\alpha) T_f}\left[e^{(\lambda+\mu)\theta T_f} - 1\right]\right\}. \tag{15}$$

It is easy to prove that the functions $\phi_{(i)}(\theta; x)$ are strictly convex in θ by considering their secondary derivations. Then, the interference metric in (2) can be reformulated as

$$\overline{I}_1 = \mathbb{E}_{\boldsymbol{\omega}}\left\{\sum_{m=1}^{M}\left[\phi_{(1)}\left(\theta_m^{(1)}(\boldsymbol{\omega}); x_m\right) + \phi_{(2)}\left(\theta_m^{(2)}(\boldsymbol{\omega}); y_m\right)\right]\right\}. \tag{16}$$

After some simple manipulations, the problem (P) can be reformulated as a convex optimization problem, i.e.,

$$\min_{\substack{P_{s,n}^{(1)}(\boldsymbol{\omega}), P_{s,n}^{(2)}(\boldsymbol{\omega}), P_{r,n}(\boldsymbol{\omega}),\\ \theta_m^{(1)}(\boldsymbol{\omega}), \theta_m^{(2)}(\boldsymbol{\omega}), n \in \mathcal{N},\ m \in \mathcal{M}}} \overline{I}_1 \tag{17}$$

$$\text{s.t.} \quad \overline{R}_1 \geq R_{\min}, \quad \overline{R}_2 \geq R_{\min} \tag{18}$$

$$\mathbb{E}_{\boldsymbol{\omega}}\left\{\sum_{n=1}^{N}\left[\overline{P}_{s,n}^{(1)}(\boldsymbol{\omega}) + P_{s,n}^{(2)}(\boldsymbol{\omega})\right]\right\} \leq P_{\max}^{s} \tag{19}$$

$$\mathbb{E}_{\boldsymbol{\omega}}\left\{\sum_{n=1}^{N} P_{r,n}(\boldsymbol{\omega})\right\} \leq P_{\max}^{r} \tag{20}$$

$$P_{s,n}^{(1)}(\boldsymbol{\omega}), P_{s,n}^{(2)}(\boldsymbol{\omega}), P_{r,n}(\boldsymbol{\omega}) \geq 0, \ n \in \mathcal{N} \tag{21}$$

$$0 \leq \theta_m^{(1)}(\boldsymbol{\omega}) \leq \alpha, 0 \leq \theta_m^{(2)}(\boldsymbol{\omega}) \leq 1 - \alpha, \ m \in \mathcal{M}, \tag{22}$$

where $\overline{R}_1, \overline{R}_2$ are determined by

$$\overline{R}_1 = W \sum_{m \in \mathcal{M}} \sum_{n \in \mathcal{N}_m} \mathbb{E}_{\boldsymbol{\omega}}\Bigg[\theta_m^{(2)}(\boldsymbol{\omega}) \log_2\left(1 + \frac{P_{s,n}^{(2)}(\boldsymbol{\omega}) g_n^{s,d}}{\theta_m^{(2)}(\boldsymbol{\omega})}\right)$$
$$+ \theta_m^{(1)}(\boldsymbol{\omega}) \log_2\left(1 + \frac{P_{s,n}^{(1)}(\boldsymbol{\omega}) \max\{g_n^{s,r}, g_n^{s,d}\}}{\theta_m^{(1)}(\boldsymbol{\omega})}\right)\Bigg], \tag{23}$$

$$\overline{R}_2 = W \sum_{m \in \mathcal{M}} \sum_{n \in \mathcal{N}_m} \mathbb{E}_{\boldsymbol{\omega}}\Bigg[\theta_m^{(1)}(\boldsymbol{\omega}) \log_2\left(1 + \frac{P_{s,n}^{(1)}(\boldsymbol{\omega}) g_n^{s,d}}{\theta_m^{(1)}(\boldsymbol{\omega})}\right)$$
$$+ \theta_m^{(2)}(\boldsymbol{\omega}) \log_2\left(1 + \frac{P_{s,n}^{(2)}(\boldsymbol{\omega}) g_n^{s,d} + P_{r,n}(\boldsymbol{\omega}) g_n^{r,d}}{\theta_m^{(2)}(\boldsymbol{\omega})}\right)\Bigg]. \tag{24}$$

B. The optimal solution of (P)

By solving the KKT conditions of the derived convex optimization problem (17)-(22), we derived the optimal solution for each realization of the NSI $\boldsymbol{\omega}$ and fixed dual variables [14]:

The optimal value of the ratio $P_{s,n}^{(1)}(\boldsymbol{\omega}) / \theta_m^{(1)}(\boldsymbol{\omega})$ is given by

$$\frac{P_{s,n}^{(1)}(\boldsymbol{\omega})}{\theta_m^{(1)}(\boldsymbol{\omega})} = \text{positive root } x \text{ of (26) if it exists, otherwise } 0, \tag{25}$$

and the root x is determined by

$$\frac{\zeta \max\{g_n^{s,r}, g_n^{s,d}\}}{1+x\max\{g_n^{s,r}, g_n^{s,d}\}} + \frac{\sigma g_n^{s,d}}{1+xg_n^{s,d}} = \varepsilon \ln 2, \tag{26}$$

which is equivalent with a quadratic equation with closed-form solutions.

The optimal values of the ratios $P_{s,n}^{(2)}(\boldsymbol{\omega})/\theta_m^{(2)}(\boldsymbol{\omega})$ and $P_{r,n}(\boldsymbol{\omega})/\theta_m^{(2)}(\boldsymbol{\omega})$ are given by

$$\frac{P_{s,n}^{(2)}(\boldsymbol{\omega})}{\theta_m^{(2)}(\boldsymbol{\omega})} = \left(\frac{\zeta}{(\varepsilon - \eta g_n^{s,d}/g_n^{r,d})\ln 2} - \frac{1}{g_n^{s,d}}\right)^+, \tag{27}$$

$$\frac{P_{r,n}(\boldsymbol{\omega})}{\theta_m^{(2)}(\boldsymbol{\omega})} = \frac{\sigma}{\eta \ln 2} - \frac{1}{g_n^{r,d}} - \frac{P_{s,n}^{(2)}(\boldsymbol{\omega})g_n^{s,d}}{\theta_m^{(2)}(\boldsymbol{\omega})g_n^{r,d}}, \tag{28}$$

with $(\cdot)^+ \triangleq \max(\cdot, 0)$, if $P_{r,n}(\boldsymbol{\omega}) > 0$ is satisfied. Otherwise, if $P_{r,n}(\boldsymbol{\omega}) = 0$, we obtain

$$\frac{P_{s,n}^{(2)}(\boldsymbol{\omega})}{\theta_m^{(2)}(\boldsymbol{\omega})} = \left(\frac{\zeta+\sigma}{\varepsilon \ln 2} - \frac{1}{g_n^{s,d}}\right)^+, \tag{29}$$

$$\frac{P_{r,n}(\boldsymbol{\omega})}{\theta_m^{(2)}(\boldsymbol{\omega})} = 0. \tag{30}$$

The optimal value of $\theta_m^{(1)}(\boldsymbol{\omega})$ is determined as

$$\begin{cases} \theta_m^{(1)}(\boldsymbol{\omega}) = \left[-\frac{1}{(\lambda+\mu)T_f}\ln\left\{1-\frac{\lambda+\mu}{\lambda}\sum_{n\in\mathcal{N}_m}\left[\sigma f\left(g_n^{s,d}\frac{P_{s,n}^{(1)}(\boldsymbol{\omega})}{\theta_m^{(1)}(\boldsymbol{\omega})}\right)\right.\right.\right. \\ \qquad \left.\left.\left. +\zeta f\left(\max\{g_n^{s,r}, g_n^{s,d}\}\frac{P_{s,n}^{(1)}(\boldsymbol{\omega})}{\theta_m^{(1)}(\boldsymbol{\omega})}\right)\right]\right\}\right]_0^{\alpha}, \text{if } x_m = 0, \\ \theta_m^{(1)}(\boldsymbol{\omega}) = \left[\alpha+\frac{1}{(\lambda+\mu)T_f}\ln\left\{\frac{\lambda+\mu}{\mu}\sum_{n\in\mathcal{N}_m}\left[\sigma f\left(g_n^{s,d}\frac{P_{s,n}^{(1)}(\boldsymbol{\omega})}{\theta_m^{(1)}(\boldsymbol{\omega})}\right)\right.\right.\right. \\ \qquad \left.\left.\left. +\zeta f\left(\max\{g_n^{s,r}, g_n^{s,d}\}\frac{P_{s,n}^{(1)}(\boldsymbol{\omega})}{\theta_m^{(1)}(\boldsymbol{\omega})}\right]-\frac{\lambda}{\mu}\right\}\right)\right]_0^{\alpha}, \text{if } x_m = 1, \end{cases} \tag{31}$$

where the value of $P_{s,n}^{(1)}(\boldsymbol{\omega})/\theta_m^{(1)}(\boldsymbol{\omega})$ is given by (25), $f(x) \triangleq \log_2(1+x) - \frac{x}{(1+x)\ln 2}$, $[x]_0^y \triangleq \min\{\max\{x, 0\}, y\}$, and $\ln(x)$ is extended to take the value $-\infty$ for $x \in (-\infty, 0]$ to simplify the formulations. The optimal value of $\theta_m^{(2)}(\boldsymbol{\omega})$ is given by

$$\begin{cases} \theta_m^{(2)}(\boldsymbol{\omega}) = \left[-\frac{1}{(\lambda+\mu)T_f}\ln\left\{1-\frac{\lambda+\mu}{\lambda}\sum_{n\in\mathcal{N}_m}\left[\zeta f\left(g_n^{s,d}\frac{P_{s,n}^{(2)}(\boldsymbol{\omega})}{\theta_m^{(2)}(\boldsymbol{\omega})}\right)\right.\right.\right. \\ \qquad \left.\left.\left. +\sigma f\left(g_n^{s,d}\frac{P_{s,n}^{(2)}(\boldsymbol{\omega})}{\theta_m^{(2)}(\boldsymbol{\omega})}+g_n^{r,d}\frac{P_{r,n}(\boldsymbol{\omega})}{\theta_m^{(2)}(\boldsymbol{\omega})}\right)\right]\right\}\right]_0^{1-\alpha}, \text{if } y_m = 0, \\ \theta_m^{(2)}(\boldsymbol{\omega}) = \left[1-\alpha+\frac{1}{(\lambda+\mu)T_f}\ln\left\{\frac{\lambda+\mu}{\mu}\sum_{n\in\mathcal{N}_m}\left[\zeta f\left(g_n^{s,d}\frac{P_{s,n}^{(2)}(\boldsymbol{\omega})}{\theta_m^{(2)}(\boldsymbol{\omega})}\right)\right.\right.\right. \\ \qquad \left.\left.\left. +\sigma f\left(g_n^{s,d}\frac{P_{s,n}^{(2)}(\boldsymbol{\omega})}{\theta_m^{(2)}(\boldsymbol{\omega})}+g_n^{r,d}\frac{P_{r,n}(\boldsymbol{\omega})}{\theta_m^{(2)}(\boldsymbol{\omega})}\right)\right]-\frac{\lambda}{\mu}\right\}\right]_0^{1-\alpha}, \text{if } y_m = 1, \end{cases} \tag{32}$$

where the values of $P_{s,n}^{(2)}(\boldsymbol{\omega})/\theta_m^{(2)}(\boldsymbol{\omega})$ and $P_{r,n}(\boldsymbol{\omega})/\theta_m^{(2)}(\boldsymbol{\omega})$ are given by (27)-(30). Substituting (31)-(32) into (25)-(30), the optimal values of $P_{s,n}^{(1)}(\boldsymbol{\omega}), P_{s,n}^{(2)}(\boldsymbol{\omega}), P_{r,n}(\boldsymbol{\omega})$ are derived.

We now optimize the dual variables $\boldsymbol{\nu} \triangleq \{\zeta, \sigma, \varepsilon, \eta\}^T$ by the subgradient method [14], where the subgradient $\boldsymbol{h}(\boldsymbol{\nu})$ at the dual point $\boldsymbol{\nu}$ is given by

$$\boldsymbol{h}(\boldsymbol{\nu}) = \begin{bmatrix} (R_{\min} - \overline{R}_1^{\star})/W \\ (R_{\min} - \overline{R}_2^{\star})/W \\ \sum_{n=1}^N \mathbb{E}_{\boldsymbol{\omega}}\left\{P_{s,n}^{(1)\star}(\boldsymbol{\omega}) + P_{s,n}^{(2)\star}(\boldsymbol{\omega})\right\} - P_{\max}^s \\ \sum_{n=1}^N \mathbb{E}_{\boldsymbol{\omega}}\left\{P_{r,n}^{\star}(\boldsymbol{\omega})\right\} - P_{\max}^r \end{bmatrix}, \tag{33}$$

where $P_{s,n}^{(1)\star}(\boldsymbol{\omega})$, $P_{s,n}^{(2)\star}(\boldsymbol{\omega})$ and $P_{r,n}^{\star}(\boldsymbol{\omega})$ are derived throught (25)-(32) at the dual point $\boldsymbol{\nu}$, and $\overline{R}_1^{\star}$ and $\overline{R}_2^{\star}$ are the corresponding rate values in (23) and (24), respectively.

C. Real-time implementations

In the following, we show that dual variable $\boldsymbol{\nu}$ can be optimized off-line, which reduces the amount of real-time computations greatly. Moreover, by utilizing the structure of the optimal solution (25)-(32), the primal solutions $\{P_{s,n}^{(1)}(\boldsymbol{\omega}), P_{s,n}^{(2)}(\boldsymbol{\omega}), P_{r,n}(\boldsymbol{\omega}), \theta_m^{(1)}(\boldsymbol{\omega}), \theta_m^{(2)}(\boldsymbol{\omega})\}$ can be updated on-line efficiently based on real-time NSI $\boldsymbol{\omega}$ of each frame, while generating quite short sensing-transmission delay.

1) Off-line dual optimization: These expectations (23), (24) and (33) do not have closed-form expressions. In practice, one can compute the subgradient $\boldsymbol{h}(\boldsymbol{\nu})$ by means of Monte Carlo simulations. Specifically, one may randomly generate a set of realizations of the NSI $\boldsymbol{\omega}$ following the distributions of the CQIs and sensing outcomes. Then, the expectation terms in (23), (24) and (33) can be obtained by computing (25)-(32), (23) and (24) for each realization of $\boldsymbol{\omega}$, and then averaging the corresponding terms in (23), (24) and (33) over these realizations. By this, the subgradient updates with high computation burden can be performed off-line without using real-time NSI.

2) On-line primal solution update: In practice, the BS (destination) acquires the CQI $\{g_n^{s,r}(l), g_n^{s,d}(l), g_n^{r,d}(l)\}_{n=1}^N$ of Frame l even before Frame l starts through prediction [16], if the wireless channel varies slowly across the frames. Therefore, the BS can compute the ratio $\frac{P_{s,n}^{(1)}(\boldsymbol{\omega}_l)}{\theta_m^{(1)}(\boldsymbol{\omega}_l)}$, $\frac{P_{s,n}^{(2)}(\boldsymbol{\omega}_l)}{\theta_m^{(2)}(\boldsymbol{\omega}_l)}$ and $\frac{P_{r,n}(\boldsymbol{\omega}_l)}{\theta_m^{(2)}(\boldsymbol{\omega}_l)}$ according to (26)-(30) in Frame $l-1$. While the sensing outcome $x_m(l)$ and $y_m(l)$ is still unknown at the BS at this moment, the BS can compute $\theta_m^{(1)}(\boldsymbol{\omega}_l)$ and $\theta_m^{(2)}(\boldsymbol{\omega}_l)$ in (31) and (32) by considering the two possible values of of $x_m(l)$ and $y_m(l)$, respectively. Then, the BS sends $\frac{P_{s,n}^{(1)}(\boldsymbol{\omega}_l)}{\theta_m^{(1)}(\boldsymbol{\omega}_l)}$, $\frac{P_{s,n}^{(2)}(\boldsymbol{\omega}_l)}{\theta_m^{(2)}(\boldsymbol{\omega}_l)}$ and the possible vales of $\theta_m^{(1)}(\boldsymbol{\omega}_l)$ and $\theta_m^{(2)}(\boldsymbol{\omega}_l)$ to the MT before Frame l starts, and sends $\frac{P_{r,n}(\boldsymbol{\omega}_l)}{\theta_m^{(2)}(\boldsymbol{\omega}_l)}$ and the possible values of $\theta_m^{(2)}(\boldsymbol{\omega}_l)$ to the relay before Phase 2 of Frame l starts.

After receiving the feedbacks from the destination, the MT performs spectrum sensing at the beginning of Phase 1, and then selects the value of $\theta_m^{(1)}(\boldsymbol{\omega}_l)$ according to the sensing outcome $x_m(l)$. After Phase 1 of Frame l, the MT and relay node perform spectrum sensing again at the beginning of Phase 2, and then selects the value of $\theta_m^{(2)}(\boldsymbol{\omega}_l)$ in accordance with the sensing outcomes $y_m(l)$. Therefore the MT and relay nodes can transmit information signals right after spectrum sensing with almost no sensing-transmission delay.

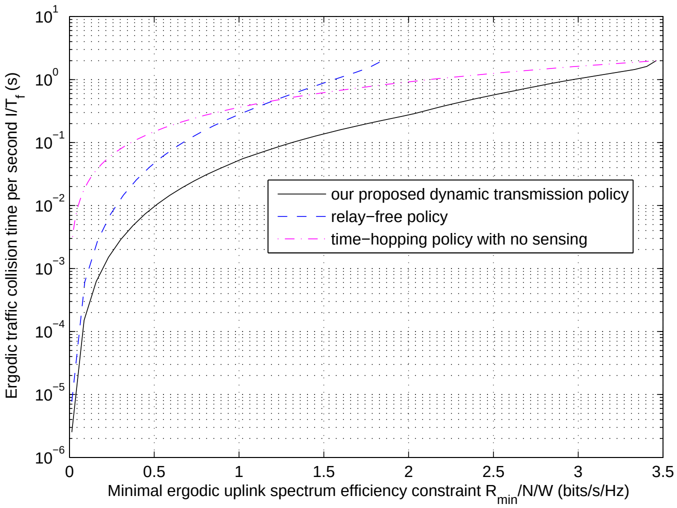

Fig. 3: The interference mitigation performance of different spectrum sharing policies.

V. Numerical experiments

We now compare our dynamic transmission policy with 2 reference policies:

1. The first one is a *relay-free policy* [10], where the source transmits signals directly to the destination without using the relay node.

2. We then consider a *time-hopping* random access policy with no spectrum sensing [17], where the CRN's transmission time is chosen randomly in each frame like frequency hopping. In this policy, the transmission time of the CRN satisfies $\theta_n^{(i)}(\boldsymbol{\omega}_l) = \theta$ for $n = 1, \ldots, N$, $i = 1, 2$ and all frame index l, and the transmission powers of the source and relay are allocated optimally to maximize $\overline{R}_{DF}$.

We consider that the source, relay and destination stands in a line and the relay locates in the middle of the source and destination. The CRN has $N = 16$ sub-channels, and the ad-hoc network has $M = 4$ bands. Thus, each ad-hoc band overlaps with 4 CRN sub-channels. The channel gain between every two nodes of the CRN at each sub-channel can be decomposed into a small-scale Rayleigh fading and a large-scaled path loss component with a path-loss factor of 4. The small-scale fading are i.i.d. across the sub-channels to simulate a frequency-selective environment. We assume that the power constraints of the source and relay nodes are the same and the signal-to-interference-plus-noise ratio (SINR) of the source-destination link is $\frac{P_{\max}^s \mathbb{E}\{g_n^{s,d}\}}{N} = 5$dB. The parameters of ad-hoc traffic model satisfy $\mu T_f = \lambda T_f = 1$. The value of α is chosen to be 0.5.

Figure 3 illustrates the interference mitigation performance of the spectrum sharing policies. We find that our policy achieves better interference mitigation performance than the reference policies. More specifically, the relay-free policy is slightly worse than our policy in low spectrum efficiency region. However, if the required uplink spectrum efficiency is relative high, the interference mitigation performance of relay-free policy is quite poor, because of its relative low capacity. The spectrum efficiency of our policy is 80% higher than that of the relay-free policy, when the ergodic traffic collision time per second is larger than 0.01s. The time-hopping policy has quite poor performance for relative low spectrum efficiency, because it has not utilized the spectrum sensing results.

VI. Conclusions

This paper studied a spectrum sharing scenario between cooperative relay and ad-hoc networks. A dynamic transmission policy of the CRN is proposed which requires little real-time computation and guarantees high traffic prediction accuracy. The benefits of spectrum sensing and cooperative relay techniques are demonstrated by our numerical experiments.

Acknowledgement

The authors would like to thank Yongle Wu, Ying Cui and Ness B. Shroff for constructive discussions about this work.

References

[1] Q. Zhao and B. M. Sadler, "A survey of dynamic spectrum access: Signal processing, networking, and regulatory policy," *IEEE Signal Process. Mag.*, vol. 24, no. 5, pp. 79–89, May 2007.

[2] V. Chandrasekhar, J. G. Andrews, and A. Gatherer, "Femtocell networks: A survey," *IEEE Commun. Mag.*, vol. 46, no. 9, pp. 59–67, Sep. 2008.

[3] S. Geirhofer, L. Tong, and B. M. Sadler, "Dynamic spectrum access in the time domain: Modeling and exploiting whitespace," *IEEE Commun. Mag.*, vol. 45, no. 5, pp. 66–72, May 2007.

[4] ——, "Cognitive medium access: Constraining interference based on experimental models," *IEEE J. Sel. Areas Commun.*, vol. 26, no. 1, pp. 95–105, Jan. 2008.

[5] Q. Zhao, S. Geirhofer, L. Tong, and B. M. Sadler, "Opportunistic spectrum access via periodic channel sensing," *IEEE Trans. Signal Process.*, vol. 56, no. 2, pp. 785–796, Feb. 2008.

[6] S. Geirhofer, J. Z. Sun, L. Tong, and B. M. Sadler, "Cognitive frequency hopping based on interference prediction: Theory and experimental results," *ACM SIGMOBILE Mob. Comput.and Commun. Rev.*, vol. 13, no. 2, pp. 49–61, Apr. 2009.

[7] Y. Xu, Y. Sun, Y. Li, Y. Zhao, and H. Zou, "Joint sensing period and transmission time optimization for energy-constrained cognitive radios," *EURASIP J. Wirel. Commun. Netw.*, vol. 2010, Article ID 818964, 16 pages, 2010.

[8] L. Lai, H. El Gamal, H. Jiang, and H. Poor, "Cognitive medium access: Exploration, exploitation, and competition," *IEEE Trans. Mob. Comput.*, vol. 10, no. 2, pp. 239–253, Feb. 2011.

[9] X. Li, Q. C. Zhao, X. Guan, and L. Tong, "Optimal cognitive access of Markovian channels under tight collision constraints," *IEEE J. Sel. Areas Commun.*, 2011, to appear.

[10] S. Geirhofer, L. Tong, and B. M. Sadler, "A sensing-based cognitive coexistence method for interfering infrastructure and ad-hoc systems," *Wirel. Commun. Mob. Comput.*, vol. 10, no. 1, pp. 16–30, Jan. 2010.

[11] Y. Sun, Y. Li, X. Zhong, S. Zhou, and X. Xu, "Resource allocation for the cognitive coexistence of ad-hoc and cooperative relay networks," in *Proceedings of IEEE International Conference on Communications (IEEE ICC 2010)*, Kempton, South Africa, May 2010.

[12] K. Huang, V. Lau, and Y. Chen, "Spectrum sharing between cellular and mobile ad hoc networks: Transmission-capacity trade-off," *IEEE J. Sel. Areas Commun.*, vol. 27, no. 7, pp. 1256–1267, Sep. 2009.

[13] S. I. Resnick, *Adventures in Stochastic processes*. Boston, MA: Birkhäuser, 1992.

[14] Y. Sun, X. Zhong, T.-H. Chang, S. Zhou, and C.-Y. Chi, "Spectrum sharing between cooperative relay and ad-hoc networks: Spectrum access, resource allocation and real-time implementation," *IEEE Trans. Signal Process.*, 2011, submitted for publication.

[15] S. Boyd and L. Vandenberghe, *Convex Optimization*. Cambridge, UK: Cambridge University Press, 2004.

[16] Y. Zhang, S. Liu, Y. Rui, S. Zhou, and J. Wang, "Channel prediction assisted by radio propagation environments information," in *Proc. IEEE Int. Conf. Circuits Syst. Commun. (IEEE ICCSC)*, Shanghai, China, Feb. 2008, pp. 733–736.

[17] V. Chandrasekhar and J. Andrews, "Uplink capacity and interference avoidance for two-tier femtocell networks," *IEEE Trans. Wireless Commun.*, vol. 8, no. 7, pp. 3498 –3509, 2009.